Clinical Neurophysiology 190 (2026) 2111953

Contents lists available at ScienceDirect

Clinical Neurophysiology

journal homepage: www.elsevier.com/locate/clinph

Beyond motor cortex: A novel relationship between associative parietal cortex and ipsilateral silent period

Costanza Iester [a,1], Alice Bellosta [b,1], Ludovico Pedullà [c], Sabrina Brigadoi [d], Monica Biggio [b], Ambra Bisio [a], Simone Cutini [d], Elena Monteleone [b], Laura Bonzano [b,e,*], Marco Bove [a,e]

[a] Department of Experimental Medicine, Section of Human Physiology, University of Genoa, Genoa, Italy
[b] Department of Neuroscience, Rehabilitation, Ophthalmology, Genetics, Maternal and Child Health, University of Genoa, Genoa, Italy
[c] Italian Multiple Sclerosis Foundation, Scientific Research Area, Genoa, Italy
[d] Department of Developmental and Social Psychology, University of Padova, Padua, Italy
[e] IRCCS Azienda Ospedaliera Metropolitana, Genoa, Italy

ARTICLE INFO

Keywords:
Ipsilateral silent period
Functional near-infrared spectroscopy
Interhemispheric inhibition

ABSTRACT

Objectives: The ipsilateral silent period (iSP) is used to study interhemispheric control of voluntary motor output. It involves a brief suppression of electromyographic (EMG) activity in a muscle during isometric contraction, triggered by Transcranial Magnetic Stimulation (TMS) over the ipsilateral primary motor cortex (M1). The aim of this study was to investigate cortical activity associated with iSP.

Methods: The study involved 28 healthy right-handed volunteers who performed maximal contractions of the left hand (unimanual) or both hands (bimanual) across conditions with and without TMS. We combined TMS to left M1 with functional Near-Infrared Spectroscopy (fNIRS) over the right hemisphere. EMG was recorded from the hand muscles to quantify the iSP.

Results: A significantly greater normalized iSP area was found in the TMS bimanual condition compared to the unimanual one, with a strong correlation between the two. fNIRS revealed higher oxyhemoglobin (HbO) concentration changes in the No TMS condition than in the TMS conditions. Specifically, TMS induced HbO decreases in motor, prefrontal, premotor, parietal, and temporal areas. Reductions in premotor and parietal areas correlated with M1 activity decrease only in unimanual condition. In TMS conditions, a positive correlation was found between fNIRS HbO values in associative parietal cortex and the normalized iSP area: the higher the HbO concentration changes, the greater the inhibition.

Conclusions: These findings show reduced M1 activity and demonstrate that a broader frontoparietal network is influenced by the transcallosal motor output.

Significance: These findings contribute to a better understanding of interhemispheric inhibition and may have implications for the study of neurological disorders.

1. Introduction

The ipsilateral silent period (iSP) is commonly used to investigate the interhemispheric control of voluntary cortical motor output. This phenomenon involves a brief suppression of voluntary electromyographic (EMG) activity in a muscle, usually in the hand, during isometric contraction, induced by focal Transcranial Magnetic Stimulation (TMS) targeting the ipsilateral primary motor cortex (M1) (Hupfeld et al., 2020). Specifically, M1 is responsible for maintaining a steady, low-level contraction in the contralateral hand muscle (the target muscle), while the ipsilateral hand remains inactive. When a TMS pulse is applied to M1 on the ipsilateral side of the target muscle, it generates a motor evoked potential (MEP) in the contralateral resting hand (see Fig. 1). This stimulation also activates glutamatergic transcallosal fibers that cross the corpus callosum to reach the contralateral hemisphere. These fibers synapse onto inhibitory GABAergic interneurons, whose activation transiently suppresses descending corticospinal drive to the target muscle (Ferbert et al., 1992; Meyer et al., 1995). The resulting inhibition

* Corresponding author at: Department of Neuroscience, Rehabilitation, Ophthalmology, Genetics, Maternal and Child Health, University of Genoa, Largo Paolo Daneo 3, 16132, Genoa, Italy.
E-mail address: laura.bonzano@unige.it (L. Bonzano).
[1] These authors contributed equally.

https://doi.org/10.1016/j.clinph.2026.2111953
Accepted 26 May 2026
Available online 30 May 2026

of ipsilateral motor output, known as iSP, manifests as a momentary interruption in muscle activity. Alternative or complementary mechanisms have also been proposed, such as the potential contribution of ipsilateral corticospinal projections, especially under conditions of strong or bilateral muscle activation (Perez and Cohen, 2008). However, iSP is predominantly interpreted as a transcallosal phenomenon mediated by interhemispheric inhibitory interactions.

The iSP is typically quantified by its duration, depth, and/or area, each of which provides insights into the degree of suppression of ipsilateral EMG activity. Higher values for these parameters indicate stronger interhemispheric inhibition. Giovanelli et al. (2009) showed that the iSP can be modulated by the activity of the other hand: voluntary motor activation of the stimulated motor cortex, ipsilateral to the target muscle, enhances the iSP area. This effect was observed during both tonic and phasic contractions of the contralateral hand (relative to the stimulated motor cortex), across varying levels of isometric contraction, and even during motor imagery (Giovannelli et al., 2009). Interestingly, the iSP is considered to arise entirely from cortical mechanisms (Wassermann et al., 1991). This view is supported by evidence in patients with corpus callosum lesions showing absent or delayed iSP and indicating that the iSP is mediated by inhibitory cortico-cortical mechanisms involving fibers in the posterior trunk of the corpus callosum (Meyer et al., 1995, 2004). Further confirmation comes from observed iSP abnormalities in individuals with callosal dysfunctions, including conditions such as multiple sclerosis (Boroojerdi et al., 1998; Schmierer et al., 2000; Lenzi et al., 2007) and schizophrenia (Bajbouj et al., 2004).

Despite its frequent use as a marker of interhemispheric inhibition, the cortical activity underlying the iSP remains poorly understood. Research has mainly focused on interactions between homologous primary motor cortices. However, previous studies have demonstrated that a single TMS pulse applied to M1 at rest induces local neuronal activation that propagates to other cortical regions (Ilmoniemi et al., 1997). Accordingly, we hypothesized that the modulation of cortical activity associated with the iSP might extend beyond the motor areas, involving additional cortical regions. In this context, functional Near-Infrared Spectroscopy (fNIRS) represents a promising tool for investigating the cortical activity associated with the iSP (Curtin et al., 2019).

The aim of this study was to investigate the cortical activity associated with the iSP in the hemisphere contralateral to the one stimulated by TMS. We hypothesized that TMS applied during maximal isometric contraction, known to elicit an iSP, would result in decreased activity in M1, reflecting inhibitory processes. Moreover, we were interested in recording cortical activity outside M1, hypothesizing that TMS would also impact further cortical regions. By comparing cortical activity during maximal isometric contractions with and without TMS, we aimed to uncover the neural mechanisms underlying maximal isometric movements and to examine how cortical activity is modulated by ipsilateral TMS to the target muscle. Additionally, we investigated cortical activity related to the iSP when both hands performed simultaneous maximal contractions. Based on previous EMG findings showing an increased iSP area during simultaneous maximal bimanual contractions (Perez et al., 2014), we hypothesized that M1 activity would be reduced during bimanual compared with unimanual contractions during TMS stimulation.

2. Methods

2.1. Participants

Forty-two right-handed healthy volunteers eligible to undergo TMS participated in this study. Twenty-eight participants (10 males and 18 females, mean age ± SD: 25.07 ± 5.64 years, range 20–43 years) underwent the main experiment, while 14 (7 males and 7 females, mean age ± SD: 23.57 ± 4.64 years, range 20–34 years) the control experiment. The study was performed according to the latest version of the Declaration of Helsinki, and the protocol was approved by the ethics committee of Azienda Ospedaliera "San Martino," Genoa, Italy (P. R.271REG2017). All participants provided written informed consent.

2.2. Experimental procedure

Participants were seated on a chair while the coil was positioned over the left hemisphere. Surface EMG activity was recorded from both the right and left abductor pollicis brevis (APB) muscles. Since the height of the optodes does not allow fNIRS and TMS to be applied simultaneously to the same target, and the TMS-induced electromagnetic field might interfere with the electronic components of fNIRS system inducing possible artifacts and posing potential heating or safety risks due to metal components, TMS was performed on the left hemisphere and

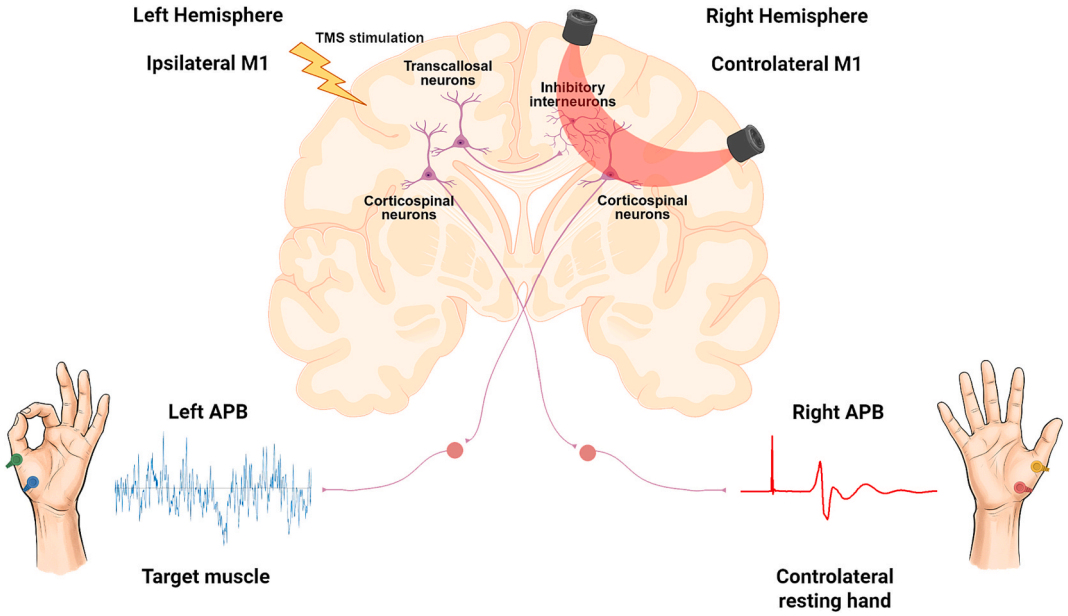

Fig. 1. Cortical mechanisms of iSP. When a TMS pulse is applied to M1 on the ipsilateral side of the target muscle, it generates a MEP in the contralateral resting hand and a brief interruption of voluntary electromyography in the target muscle during an isometric contraction.

fNIRS data were acquired only over the right hemisphere. Participants were instructed to maximally contract the target muscle of the left hand or both hands, depending on the experimental condition, by pressing the thumb against the medial edge of the index finger, without flexing the intermediate or distal phalanges. Specifically, they underwent three conditions: maximal contraction of the left hand without TMS stimulation (No TMS), maximal contraction of the left hand with TMS stimulation (TMS unimanual), and maximal contraction of both hands with TMS stimulation (TMS bimanual). The No TMS condition was used as the reference condition, with the coil placed on the scalp but no stimulation delivered. In the TMS conditions, stimulation was applied 1–2 s after the trial began. Trial onset coincided with the beginning of muscle contraction instructed by the experimenter. EMG and fNIRS signals were recorded during all conditions. The conditions were presented in a randomized order across participants, with 25 trials per condition (task duration: ~2 s; rest duration: ~20 s), for a total of 75 trials (see Fig. 2). At the start of the experiment, the fNIRS montage and EMG electrode placement were performed, with an average setup time of approximately 30 min.

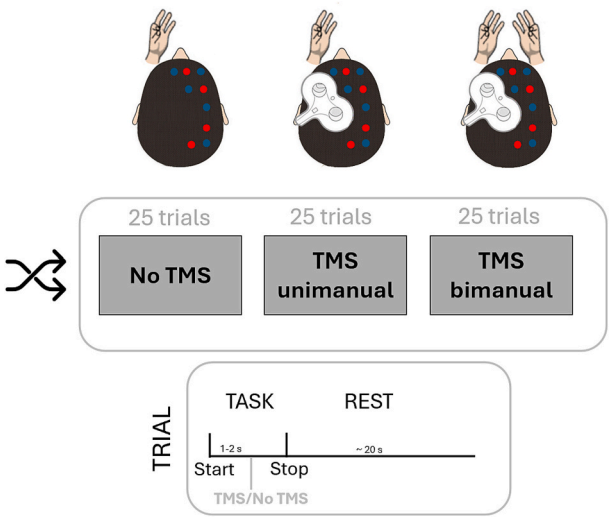

Fig. 2. Three experimental conditions were assessed in a randomized order across participants. Each condition included 25 trials. During each trial, participants were instructed to perform maximal isometric contractions using either the left hand alone or both hands simultaneously. In the TMS conditions, stimulation was applied 1–2 s after the trial began.

2.3. TMS protocol

Single pulse TMS was delivered using a 70 mm figure-of-eight connected to a Magstim 200 stimulator (Magstim Co. Whitland, UK). EMG signals were digitalized, amplified and filtered (30 Hz–3 kHz) using a D360 amplifier (Digitimer Ltd., Welwyn Garden City, Hertfordshire, UK) controlled by the Power1401-3A acquisition interface (Cambridge Electronic Design Limited, Cambridge, UK) and stored on a personal computer for display and later offline data analysis. The coil was positioned, tangentially to the scalp, over M1 with the handle pointing backwards and rotated 45 degrees from the midline perpendicular to the central sulcus. The center of the coil junction was positioned over the hand area of the left M1. First, suprathreshold stimulations were performed at different sites, and the site with the highest averaged APB response (peak-to-peak amplitude of the MEP) was identified as the hotspot for eliciting MEPs in the contralateral APB. Next, the Resting Motor Threshold (RMT) was determined for each participant as the lowest stimulator output intensity required to elicit 5 out of 10 MEPs with a peak-to-peak amplitude $\geq$ 50 μV during muscle relaxation. Finally, to assess the iSP, the stimulation intensity was increased to 120% of the RMT, and twenty-five single pulses were delivered to the left M1 for each TMS condition.

2.4. EMG acquisition and analysis

To measure EMG activity the skin was prepared, and cup surface electrodes were applied over the right and left belly of the APB muscles, and the reference electrodes were positioned on the metacarpophalangeal joint of the thumb of both hands. The ground electrode was placed on one of the styloid processes.

To obtain the iSP, EMG signals were analyzed using custom software developed in MATLAB (MathWorks, MA, USA). Since there was no stimulation in the No TMS condition, the iSP was computed only for two out of the three conditions (TMS unimanual and TMS bimanual).

For each participant and condition, the iSP was identified on single-trial rectified EMG traces from the left hand. For each trial, we verified whether the EMG signal fell below the mean pre-stimulus amplitude (calculated over the 90 ms window preceding the TMS pulse) for at least 10 ms within the 25–75 ms post-stimulus window. Trials that did not meet this criterion were discarded from further analysis; however, these represented less than 6% of all trials.

The selected rectified EMG traces were then averaged, and the result was used to identify the iSP. The pre-stimulus mean EMG level was calculated over a 90 ms window immediately preceding the TMS pulse, corresponding to the initial phase of maximal isometric contraction. Over the same interval, the area under the pre-stimulus EMG signal was calculated. Specifically, the iSP was evaluated in terms of normalized iSP area, based on the following parameters: the onset and offset of the iSP, defined as the points after cortical stimulation where EMG activity fell below and then rose up the mean amplitude of the pre-stimulus EMG activity for at least 10 ms; and the duration of the iSP, determined by the time elapsed between the iSP onset and offset. The normalized iSP area was then calculated using the following formula:

$$NormalizediSParea = \frac{[(prestimulusmeanEMG \times iSPduration) - (areaundertheiSP)]}{areaunderprestimulusEMG}$$

where pre-stimulus mean EMG refers to the average of the rectified EMG signal during the pre-stimulus baseline, measured in millivolts (mV); iSP duration is the length of the silent period, expressed in milliseconds (ms); the area under the iSP is the integral of the rectified EMG signal during the iSP window, expressed in millivolts per millisecond (mV × ms); and the area under pre-stimulus EMG refers to the integral of the rectified EMG signal in the pre-stimulus time interval (mV × ms). The resulting value is dimensionless and represents the proportion of EMG suppression relative to baseline activity. The normalized iSP area is a stable measure and is independent of the level of contraction in the ipsilateral muscles (Trompetto et al., 2004). Notably, the normalized iSP area can become equivalent to the average iSP depth when the pre-stimulus EMG area is computed over the same duration as the iSP. However, in this study the pre-stimulus time interval is always larger than iSP duration.

2.5. fNIRS acquisition

Using a continuous-wave, portable, multichannel NIRS system (NIRSport 2, NIRx Medical Technologies, Berlin, Germany), fNIRS data were collected. The system included 16 LED illumination sources and 16 detection sensors, which operated at two wavelengths of near-infrared light (760 nm and 850 nm) to monitor changes in oxyhemoglobin (HbO) and deoxyhemoglobin (HbR) concentrations. Participants wore a flexible black cap (EasyCap, Germany) with optodes positioned to cover multiple areas in the right hemisphere and only the prefrontal region of the left hemisphere due to TMS-related spatial constraints and the limited number of available optodes. The participant's head circumference was measured so that the cap size could be selected accordingly. The array consisted of 35 standard channels with 3 cm spacing and 8 short-separation (SS) channels with 8 mm spacing. The correct channel placement was ensured by using an fNIRS cap with 10–10 international EEG system references. The Vertex (Cz in EEG references) was located at the midpoint between the Nasion, Inion, and the ear tragus points for accurate positioning.

2.6. fNIRS analysis

For each participant, the pre-processing of fNIRS signals was conducted using MATLAB (MathWorks, MA, USA) with custom scripts and selected functions from the Homer3 NIRS processing package (Huppert et al., 2009). Channels exhibiting a low signal-to-noise ratio (SNR < 2) or very low optical intensity were excluded from further analysis, while the intensity data from the remaining channels were converted to changes in optical density. Motion artifacts were corrected using a combination (Di Lorenzo et al., 2019) of spline ($p = 0.99$) (Scholkmann et al., 2010; Yücel et al., 2014) and the wavelet motion correction technique ($iqr = 0.5$), as described by Molavi and Dumont (2012), and any residual motion artifacts were identified using the hmrR_MotionArtifact (tmotion $= 0.5$, tMask $= 1$, STDtrresh $= 12.0$, AMPthresh $= 0.5$) function. Trials containing these artifacts within a time window of -2 s to 3 s post-task onset were discarded. The proportion of rejected trials was negligible (No TMS: 1.71%, unilateral TMS: 1.28%, bilateral TMS: 0.43%), corresponding to fewer than one discarded trial per condition on average. This indicates that motion artifacts were minimal and effectively mitigated during preprocessing. To eliminate slow drifts and high-frequency noise, a band-pass filter (0.01–3 Hz) was applied. Each participant's age-dependent differential pathlength factor was computed according to Scholkmann and Wolf (2013). HbO and HbR concentration changes were then determined using the modified Beer-Lambert law (Delpy, 1988). The mean hemodynamic response function (HRF) for each task block, participant, and channel was estimated through a General Linear Model (GLM) approach solved via an iterative weighted least squares method (Barker et al., 2013). Temporal basis functions for the HRF were represented by a series of Gaussian profiles with a spacing of 1 s and a standard deviation of 2 s. The block average interval for HRF computation spanned from -2 to 15 s. Thus, 2 s before the beginning of the task were used as baseline.

To mitigate physiological noise, for each standard channel, the most correlated SS channel was added as additional regressor in the GLM design matrix (see Fig. S1). Finally, HRFs from channels associated to the same Brodmann area (BA) were averaged, resulting in HRFs for 17 regions of interest (see Table S1). The anatomical localizations of the channels were determined using the Brodmann brain atlas in the fNIRS Optodes' Location Decider (fOLD) toolbox (Zimeo Morais et al., 2018).

2.7. Statistical analysis

All Statistical analyses were performed using STATISTICA (StatSoft, Inc., 2011, STATISTICA Data Analysis Software System).

2.7.1. EMG statistical analysis

The comparison of normalized iSP areas between TMS unimanual and TMS bimanual conditions was performed using a two-tailed paired *t*-test. To characterize the relationship between the two measures, we conducted a linear regression analysis, which also provides the corresponding correlation coefficient.

2.7.2. fNIRS statistical analysis

For each participant, condition, and BA, the average HRFs for HbO and HbR between 2 and 6 s after contraction onset were calculated and used as metrics for statistical analysis. Active BAs were identified as those regions showing significant positive changes in HbO concentration (using a one-tailed *t*-test with Bonferroni correction for multiple comparisons) and significant negative changes in HbR concentration (using a one-tailed *t*-test with Bonferroni correction for multiple comparisons). Only BAs found to be active during at least one condition were included in further statistical analyses. To assess differences among the three conditions, HbO and HbR concentration changes were analyzed separately with two repeated measures ANOVA, with Condition (with 3 levels: No TMS, TMS unimanual, TMS bimanual) and BA (with 17 levels: active BAs) as within-subject factors. Post-hoc comparisons were conducted using Newman-Keuls test.

Then, we calculated the difference in HbO concentration changes between No TMS and TMS unimanual condition, as well as between No TMS and TMS bimanual condition ($\Delta BA_{TMS\ unimanual}$ and $\Delta BA_{TMS\ bimanual}$, respectively), specifically for the BAs showing a statistically significant difference in at least one TMS condition compared to the No TMS condition. This difference reveals the impact of iSP on the hemodynamics of the specific cortical area. In particular, we were interested in studying the relationship between the reduction in the primary motor cortex (BA4) and the selected areas. Since TMS stimulation was delivered on the left BA4, we hypothesized a reduction in the homologous right BA4 due to the transcallosal pathway. For this reason, BA4 was considered our target region. Thus, for each TMS condition, we performed the Pearson's correlation between the right ΔBA4 and the right ΔBAi (where i indicates the selected BAs). A significant positive correlation indicates an association between the reduction in activity in BA4 and the reduction in activity in the other BA. All correlations were corrected using the Bonferroni correction for multiple comparisons ($p =$ 0.05/number of selected BAs).

Finally, for each BA, we calculated Pearson's correlation coefficient between HbO concentration changes and the normalized iSP area using data from both TMS conditions together in a single analysis. All correlations were corrected using the Bonferroni correction for multiple comparisons ($p = 0.05$/number of BAs).

2.8. Control experiment

To better interpret the results of the main study, we also conducted a control experiment that differed from the main experiment only in that a new condition was introduced. This fourth condition aimed to evaluate cortical activity during maximal isometric movements performed with both hands in the absence of TMS stimulation. Based on the literature, we expected a reduction in activity in the contralateral primary motor cortex, consistent with the mechanisms of interhemispheric inhibition observed during unimanual and bimanual movements (Sohn et al., 2003; Stinear and Byblow, 2004; Soteropoulos and Perez, 2011). Specifically, during bimanual contraction without TMS, inhibitory mechanisms acting bilaterally between BA4s are presumed to be already present. Therefore, this condition allowed us to test whether the inhibitory effect induced by TMS during unimanual contraction can be achieved endogenously during bimanual contraction, without the need for external stimulation.

The experimental procedure followed that of the main experiment, with the exception that only BA4 was investigated and participants underwent four conditions: maximal contraction of the left hand

without TMS stimulation (No TMS unimanual), maximal contraction of left hand with TMS stimulation (TMS unimanual), maximal contraction of both hands without TMS stimulation (No TMS bimanual), and maximal contraction of both hands with TMS stimulation (TMS bimanual). Data were analyzed using a repeated-measures ANOVA with Condition (four levels: No TMS unimanual, TMS unimanual, No TMS bimanual, TMS bimanual) as a within-subject factor. Post-hoc comparisons were performed using the Newman–Keuls test.

3. Results

3.1. EMG results

The normalized iSP area was significantly greater in the TMS bimanual condition than in the TMS unimanual condition (mean ± SD, TMS unimanual: 0.065 ± 0.041, TMS bimanual: 0.094 ± 0.049, $t(27) = -5.23$, $p < 0.0001$, Cohen's $d = -0.991$, 95% CI [–1.44, –0.530]). Moreover, a strong linear relationship emerged between the normalized iSP areas in the two conditions, as indicated by the correlation coefficient derived from the regression model ($r = 0.81$, $p < 0.001$) (see Fig. 3): the higher the normalized iSP area in the TMS unimanual condition, the higher the normalized iSP area in the TMS bimanual condition. The linear regression analysis also revealed a slope of 0.98 ($t = 7.02$, $p < 0.001$, 95% CI [0.69, 1.27]) and an intercept of 0.03 ($t = 2.81$, $p = 0.009$, 95% CI [0.008, 0.052]). A slope close to 1 indicates a near-identical relationship between the two variables, with changes in one variable closely matching those in the other. The positive intercept suggests an offset, with the y-variable being slightly greater than the x-variable across the range of data.

3.2. fNIRS results

All BAs were found to be active in at least one condition. Fig. 4 shows the HRF for each BA. Exploring differences in HbO concentration changes, a significant main effect of the Condition factor ($F_{(2,54)} = 10.47$, $p < 0.001$, $\eta^2p = 0.28$, 95% CI [0.0819, 0.434]), the BA factor ($F_{(16,432)} = 5.88$, $p < 0.001$, $\eta^2p = 0.18$, 95% CI [0.0129, 0.213]) and the interaction Condition*BA ($F_{(32,864)} = 1.76$, $p = 0.006$, $\eta^2p = 0.06$, 95% CI [0.00195, 0.500]) were found. The Condition effect revealed that in the No TMS condition significantly higher activation was found compared to the TMS conditions (No TMS vs. TMS unimanual: 0.067 μM vs. 0.047 μM, $p < 0.001$; No TMS vs. TMS bimanual: 0.067 μM vs. 0.054 μM, $p = 0.005$), while no statistically significant difference was observed between the two TMS conditions (TMS unimanual vs. TMS bimanual: 0.047 μM vs. 0.054 μM, $p = 0.115$). The interaction effect revealed differences among conditions in specific areas (see Fig. 5), as reported in Table 1. Exploring differences in HbR concentration changes, neither the Condition factor ($F_{(2,54)} = 0.655$, $p = 0.523$, $\eta^2p = 0.0237$, 95% CI [0, 0.123]) nor the interaction Condition*BA ($F_{(32,864)} = 0.706$, $p = 0.888$, $\eta^2p = 0.0255$, 95% CI [0, 0.00822]) reached significance. Only a significant main effect of the BA factor ($F_{(16,432)} = 10.57$, $p < 0.001$, $\eta^2p = 0.28$, 95% CI [0.188, 0.322]) was observed, but it is worth noting that HbR responses were consistent with those observed with HbO, suggesting the presence of a genuine, cortically originated hemodynamic activity.

In each TMS condition, Pearson's correlation analysis was performed using the difference in HbO concentration changes relative to the No TMS condition (i.e., ΔBA = No TMS minus TMS unimanual or No TMS minus TMS bimanual). Specifically, correlation coefficients were calculated between ΔBA4 (primary motor cortex) and ΔBA9, ΔBA8 (prefrontal cortex), ΔBA6 (premotor cortex), ΔBA7 (parietal cortex), and ΔBA22 (superior temporal cortex). In the TMS unimanual condition, a statistically significant correlation was found between ΔBA4 and ΔBA8, ΔBA6, ΔBA7 (ΔBA4-ΔBA8: $r = 0.67$, $p < 0.001$; ΔBA4-ΔBA6: $r = 0.69$, $p < 0.001$; ΔBA4-ΔBA7: $r = 0.51$, $p = 0.006$; see Fig. 6A, B, C). In the TMS bimanual condition, the only statistically significant correlation

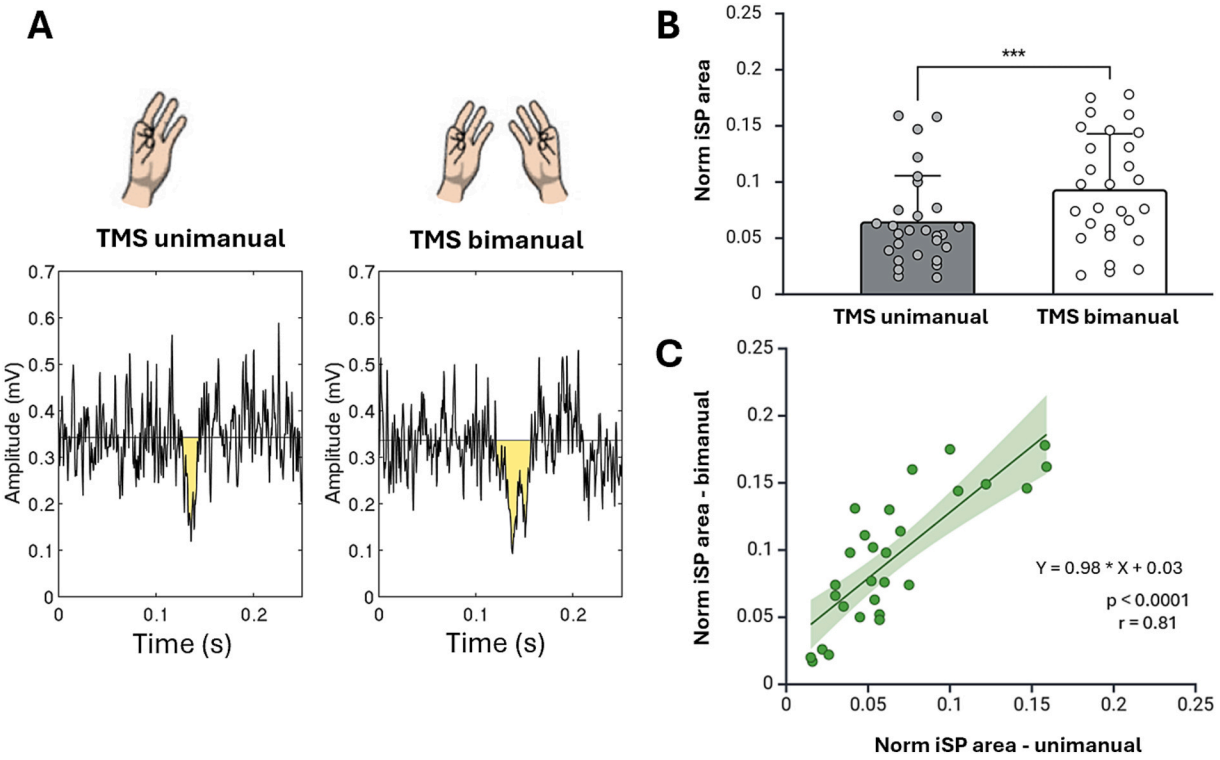

Fig. 3. A) EMG traces from a representative participant in the two TMS conditions. The normalized iSP area is filled in yellow. B) Bar plots of the normalized iSP areas in the two TMS conditions, averaged across all participants; error bars represent standard deviation (Created in https://BioRender.com). C) Linear relationship between the normalized iSP areas in the two TMS conditions (Created in https://BioRender.com). (For interpretation of the references to colour in this figure legend, the reader is referred to the web version of this article.)

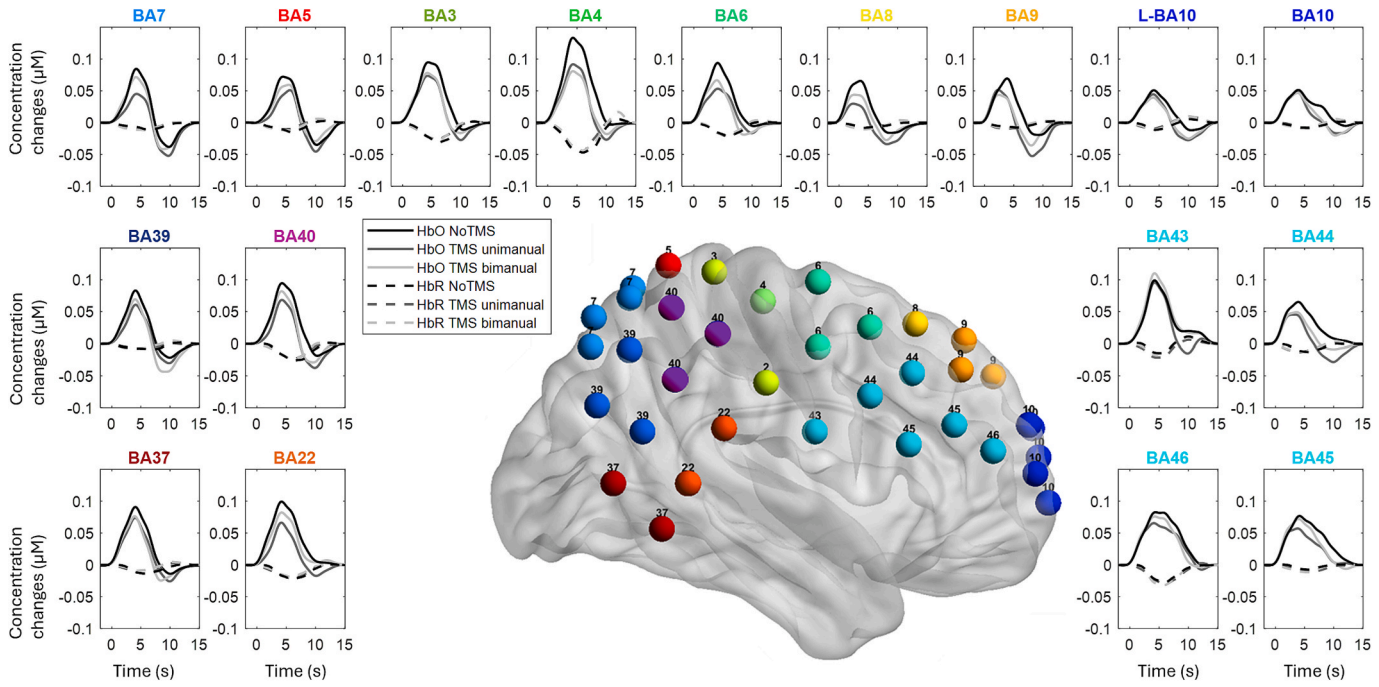

Fig. 4. Hemodynamic response functions (HRFs) for all the investigated Brodmann areas (BAs). The No TMS condition is shown in black, the TMS unimanual condition in dark grey, and the TMS bimanual condition in light grey. Solid lines represent changes in oxyhemoglobin (HbO) concentrations, while dashed lines indicate changes in deoxyhemoglobin (HbR) concentrations. The TMS pulse responsible for the iSP was applied between 1–2 s from the onset of the isometric contraction (t = 0 s). The central surface template displays the channel locations, with channels grouped by color according to their corresponding BA and labeled for clarity.

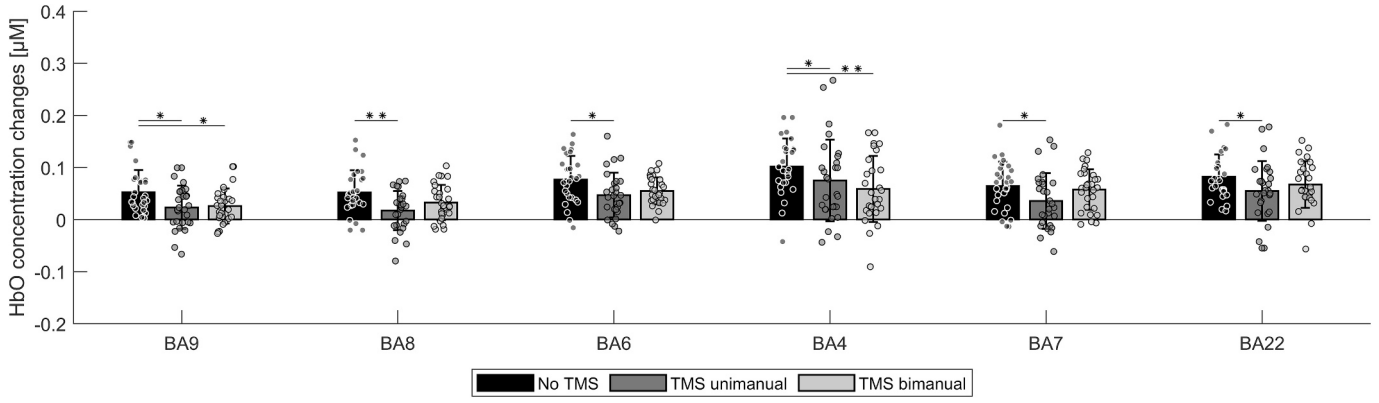

Fig. 5. Bar plots illustrating the mean values of HbO concentration changes for each Brodmann area (BA) that showed significant differences across conditions. The No TMS condition is represented in black, the unimanual TMS condition in dark grey, and the bimanual TMS condition in light grey. Error bars indicate standard deviation, * indicate $p < 0.05$, ** indicate $p < 0.001$.

was found between ΔBA4 and ΔBA6 (ΔBA4-ΔBA6: $r = 0.66$, $p < 0.001$; Fig. 6D).

Finally, only Pearson's correlation analysis between HbO concentration changes in BA5 (associative parietal cortex) and the normalized iSP area revealed a statistically significant positive correlation ($r = 0.47$, $p < 0.001$) (see Fig. 7).

3.3. Control experiment

BA4 was active in each condition. Exploring differences in HbO concentration changes, a significant main effect of the Condition factor ($F_{(3,39)} = 8.20$, $p = 0.002$, $\eta^2p = 0.39$, 95% CI [0.116, 0.534]). Post-hoc analysis revealed that BA4 was significantly higher in the No TMS unimanual condition compared to the No TMS bimanual condition (No TMS unimanual vs. No TMS bimanual: 0.112 μM vs. 0.060 μM, $p = 0.001$), and the TMS conditions (No TMS unimanual vs. TMS bimanual: 0.112 μM vs. 0.048 μM, $p < 0.001$; No TMS unimanual vs. TMS unimanual: 0.112 μM vs. 0.054 μM, $p = 0.001$), while no statistically significant difference was observed between the other conditions (TMS unimanual vs. TMS bimanual: 0.054 μM vs. 0.048 μM, $p = 0.721$; TMS unimanual vs. No TMS bimanual: 0.054 μM vs. 0.060 μM, $p = 0.673$; No TMS bimanual vs. TMS bimanual: 0.060 μM vs. 0.048 μM, $p = 0.714$) (see Fig. 8). Exploring differences in HbR concentration changes, the Condition factor ($F_{(3,39)} = 1.88$, $p = 0.149$, $\eta^2p = 0.126$, 95% CI [0, 0.279]) did not reach significance. However, as in the main experiment, the HbR responses were consistent with those observed with HbO, suggesting the presence of a genuine, cortically originated hemodynamic activity.

Table 1
Mean HbO values (μM) and standard deviation for Brodmann areas (BAs) that showed significant differences (p_values<0.05) between conditions (No TMS vs. TMS unimanual and No TMS vs. TMS bimanual).

BA	No TMS (mean ± SD)	TMS unimanual (mean ± SD)	Comparison (No TMS vs. unimanual, p_values)	TMS bimanual (mean ± SD)	Comparison (No TMS vs. bimanual, p_values)
BA9	0.0524 ± 0.0428	0.0233 ± 0.0418	0.0113	0.0259 ± 0.0337	0.0369
BA8	0.0518 ± 0.0427	0.0171 ± 0.0377	<0.001	–	–
BA6	0.0768 ± 0.0454	0.0468 ± 0.0431	0.0169	–	–
BA4	0.1014 ± 0.0539	0.0748 ± 0.0783	0.0072	0.0587 ± 0.0633	<0.001
BA7	0.0642 ± 0.0466	0.0355 ± 0.0535	0.0230	–	–
BA22	0.0823 ± 0.0426	0.0547 ± 0.0574	0.0471	–	–

4. Discussion

In this study, we combined TMS and fNIRS to investigate the iSP and its associated cortical activity. TMS applied to the hemisphere ipsilateral to the target muscle during maximal isometric contraction induced reduced activity in specific cortical regions compared to the condition without TMS, highlighting the cortical modulation elicited by TMS during sustained motor activity. Additionally, we examined cortical activity during simultaneous maximal bimanual contractions, which showed a distinct activation pattern compared to the unimanual contraction without TMS. Although no direct differences emerged between the TMS conditions, they differed in unique ways from the No TMS condition, suggesting the engagement of a partially different cortical network.

From an EMG perspective, we observed higher inhibition (i.e., a greater normalized iSP area) in the TMS bimanual than in the TMS unimanual condition, in line with the existing literature (Giovannelli et al., 2009). Then, we reported for the first time that individuals with greater normalized iSP area during the TMS unimanual condition also showed greater iSP during the TMS bimanual condition. In particular, the slope of the regression was close to one, showing that the normalized iSP area in the bimanual condition increased proportionally, with a consistent additive shift, compared to the unimanual condition. From a cortical perspective, a maximal isometric contraction of the left hand elicited increases HbO concentration changes not only in the motor cortex, but also in the prefrontal, premotor and parietal areas, consistent with evidence of a frontoparietal network supporting isometric force production (Ehrsson et al., 2000; Kuhtz-Buschbeck et al., 2008). For example, Ehrsson and colleagues showed that a precision grip activates both M1s as well as frontoparietal areas, and van Duinen et al. (2008) reported the recruitment of frontal and parietal areas during isometric contraction of the first dorsal interosseous muscle, independently of the

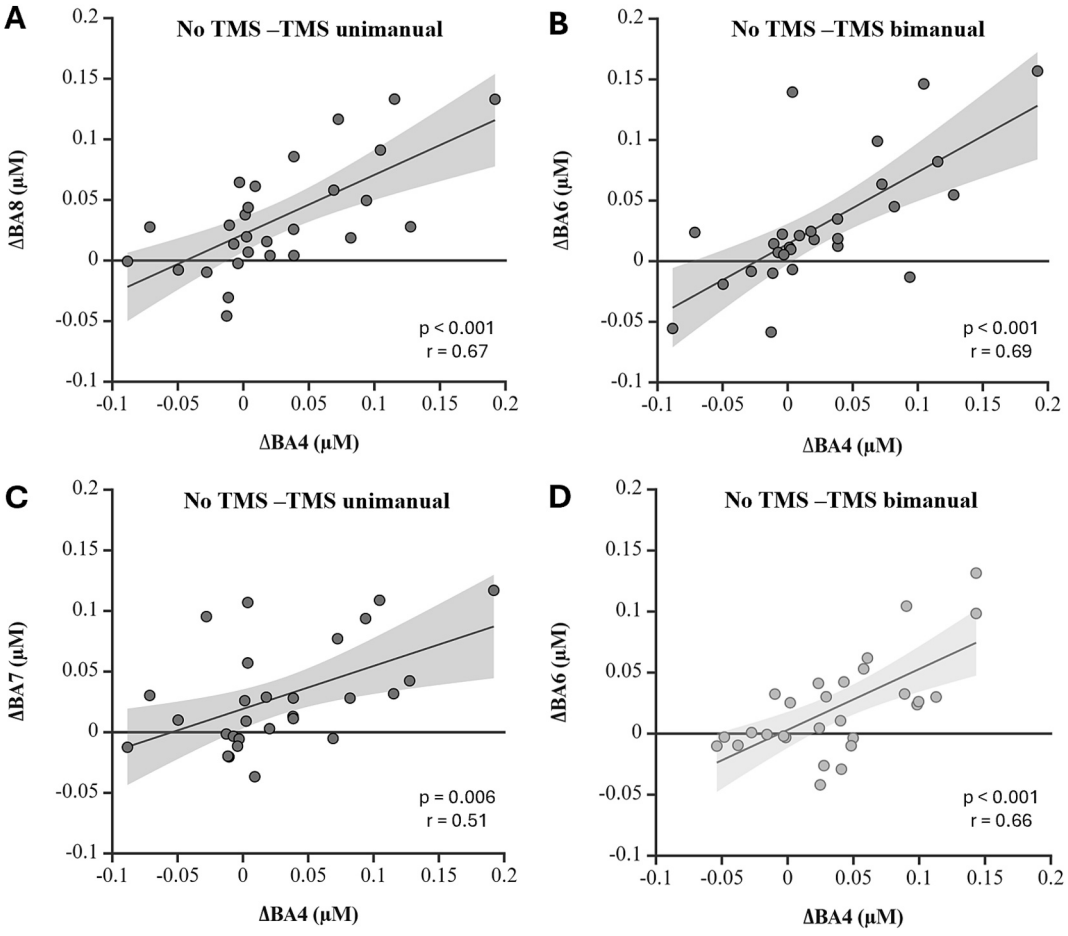

Fig. 6. Correlation between ΔBA4 and ΔBA8 in unimanual condition (A), ΔBA4 and ΔBA6 in unimanual condition (B), ΔBA4 and ΔBA7 in unimanual condition (C) and ΔBA4 and ΔBA6 in bimanual condition (D).

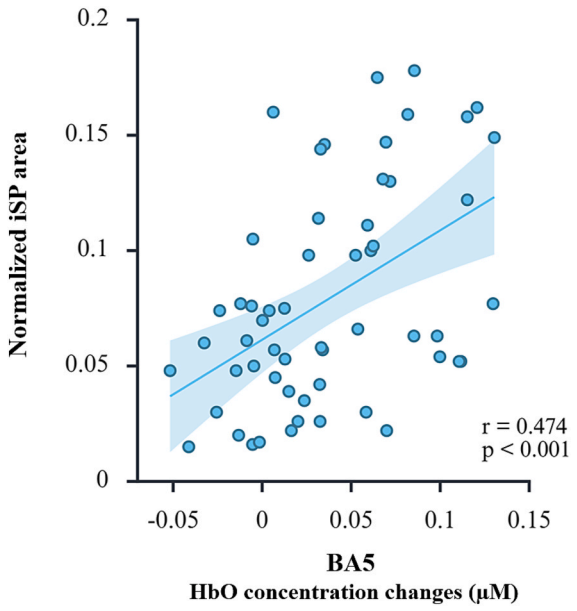

Fig. 7. Relationship between the normalized iSP area and changes in HbO concentration in BA5 (Created in https://BioRender.com).

contraction intensity. Together, these results support the role of frontoparietal system in coordinating and monitoring isometric motor output.

Then, with fNIRS we have been able to investigate how the hemodynamic responses of the right hemisphere could be modulated by the TMS stimulation of the left hemisphere during maximal isometric contraction of the left hand. We observed a decrease in HbO concentration changes that could be interpreted as a hemodynamic correlate of the interhemispheric inhibition that takes place during iSP. Specifically, the decrease was found not only in the primary motor area (BA4) but also in the prefrontal (BA9, BA8), premotor (BA6), parietal (BA7) and temporal (BA22) areas. However, it is challenging to provide a detailed explanation of these results, as there is limited literature in this field that investigates cortical activity. To our knowledge, there is only one study which investigates cortical activity related to the iSP (Bortoletto et al., 2021). They combined TMS and EEG to assess the relationship between transcallosal conduction delay and behavioral performance. However, due to EEG features, they investigated temporal features of interhemispheric communication, while a thorough understanding of the cortical correlates in terms of specific activated areas is still lacking. Previous studies have shown that TMS not only alters activity at the cortical stimulation site but also affects remote cortical regions that are functionally connected (Paus et al., 1997; Siebner et al., 1998; Fox et al., 2006; Laird et al., 2008). Interestingly, Momi and colleagues combined TMS-EEG coregistration with computational modelling to further clarify temporal dynamics among brain regions demonstrating the existence of re-entrant network activity across connected brain regions (Momi et al., 2023).

Interestingly, the reduction in activity in BA8, BA6, and BA7 correlated with the decrease in BA4 activity, whereas no such correlation was observed for BA9 and BA22. Since TMS induced both direct and indirect changes in brain activity (Siebner et al., 2022), we can hypothesize that the group of areas which showed a correlation is directly linked to BA4 inhibition. However, we cannot exclude the possibility that the signal from the left BA4 propagates through other regions of the left hemisphere before reaching the right hemisphere. Additionally, TMS can indirectly activate the brain through afferent neuronal pathways triggered by concurrent auditory and somatosensory stimulation (Siebner et al., 1999; Bestmann et al., 2004). This might explain the lack of correlation between BA4 and BA9 and BA22.

We gained valuable insights also from the TMS bimanual condition. First, BA4 showed reduced activity compared to the No TMS condition. However, we did not find a statically significant difference between TMS unimanual and TMS bimanual conditions in BA4. This contrasts with our hypothesis of a higher HbO decrease during bimanual compared unimanual TMS condition, following the increase in the normalized iSP area. These findings suggest that regions beyond BA4 may also contribute to behavioral outcomes, as demonstrated by differences between No TMS and TMS conditions. Notably, the control experiment revealed that BA4 activity in the No TMS bimanual condition was already reduced and comparable to that observed during TMS conditions, suggesting that, during bimanual contractions, endogenous inhibitory mechanisms are already active at the BA4 level, probably

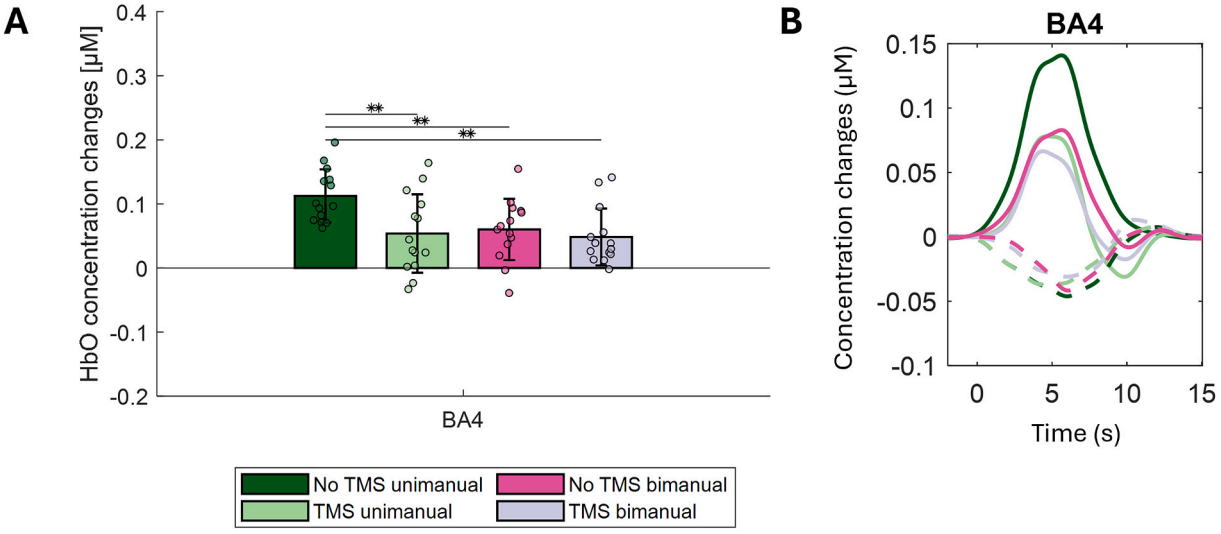

Fig. 8. Control experiment: (A) Bar plots illustrating the mean values of HbO concentration changes for Brodmann area 4. The No TMS unimanual condition is represented in dark green, the TMS unimanual condition in light green, the No TMS bimanual condition in pink, and the TMS bimanual condition in lilla. Error bars indicate standard deviation, ** indicate $p < 0.001$. (B) Hemodynamic response function (HRF) for Brodmann areas 4. Solid lines represent changes in oxyhemoglobin (HbO) concentrations, while dashed lines indicate changes in deoxyhemoglobin (HbR) concentrations. The TMS pulse responsible for the iSP was applied between 1–2 s from the onset of the isometric contraction (t = 0 s). (For interpretation of the references to colour in this figure legend, the reader is referred to the web version of this article.)

mediated by the massive recruitment of inhibitory interneurons. Specifically, the control experiment showed that there is a reduction in M1 activity when switching from unimanual to bimanual conditions, consistent with existing literature (Ortu et al., 2008). Consequently, the absence of further differences between the TMS unimanual and TMS bimanual conditions could reflect a floor effect, in which the inhibitory system has already reached a maximum level of activation.

Interestingly, although in the TMS bimanual condition there was not a statistically significant reduction in the premotor area (BA6) compared to the No TMS condition, we found a significant correlation between the reduction in BA4 and BA6 in both TMS conditions. We can assume that, during the TMS unimanual condition, reduced BA4 activity drives the decrease in BA6 through their reciprocal interaction (Sarfeld et al., 2012). In contrast, during the TMS bimanual condition, multiple factors can influence BA6 activity. TMS induces interhemispheric inhibition via callosal pathways, reducing right BA4 and consequently BA6. However, BA6 receives also a positive contribution from the left BA6 via callosal pathways (Bestmann et al., 2008). In literature, it has been shown that the anterior part of the corpus callosum, also connecting premotor areas, has a significant role in bimanual coordination tasks (Bonzano et al., 2008). These contributions may explain why the overall BA6 activity does not show a statistically significant difference compared to the No TMS condition (see Fig. 9).

Finally, in TMS conditions, we obtained a significative positive correlation between the normalized iSP area and HbO values in associative parietal cortex (BA5): the greater the normalized iSP area, the higher the HbO values. Given that greater normalized iSP area indicates greater inhibition, this finding suggests that stronger inhibition is linked to increased oxygen demand in BA5. BA5 activity has previously been associated with processes such as tactile motion discrimination, finger tracking, and finger pointing preparation (Premji et al., 2011), indicating a central role in action planning and sensorimotor integration. It is interesting to note that this region has been proposed as evolutionarily relevant for the acquisition of fine manual manipulation skills (Padberg et al., 2007), and that it may provide crucial neural signals for modulating cortical output directed to the muscles of the hand.

Anatomically, BA5 is located in the medial superior parietal lobe, and it is likely connected to ipsilateral BA4 via the superior longitudinal fasciculus (Makris et al., 2005). Functionally, BA5 can modulate the excitability of BA4 directed to the hand, probably through interactions with corticospinal neurons within BA4. Alternatively, BA5 could influence the output of BA4 indirectly, through other cortical regions. In particular, BA5 has dense projections to the premotor cortex and supplementary motor area, both of which in turn project to BA4 via the superior longitudinal fasciculus (Premji et al., 2011).

However, the observed correlation cannot be interpreted as evidence of a causal relationship. Increased BA5 activity may either contribute to interhemispheric inhibition (feedforward hypothesis) or could participate in the processing of feedback signals related to the inhibitory state of the motor system (feedback hypothesis). Distinguishing between these two hypotheses will require future studies with targeted experimental designs capable of dissociating the processes of inhibition generation from those of monitoring and sensorimotor integration.

The present findings may have important implications for the interpretation of iSP alterations reported in neurological conditions characterized by callosal demyelination, such as multiple sclerosis (MS) (Boroojerdi et al., 1998; Manson et al., 2006). Our observation that iSP-related inhibition is associated with reduced activity across a distributed frontoparietal network, rather than being confined to homologous primary motor cortices, suggests that iSP abnormalities in MS may reflect large-scale network dysfunction (Rocca et al., 2012). The present results are compatible with those reported in the study on MS (Jung et al., 2006), in which iSP does not emerge as a direct and unambiguous marker of callosal conduction dysfunction. However, the weak relationship they found between iSP abnormalities and callosal structural damage might reflect the contribution of other white matter fibers bundles such as the superior longitudinal fasciculus demonstrated to be damaged in MS (Bonzano et al., 2014), connecting also BA4 and somatosensory/spatial processing areas such as BA5. This can be supported by the significant relationship we found between BA5 activity and iSP area. Within this framework, the cortical signatures identified here in healthy individuals may provide a valuable reference for future studies aimed at investigating altered interhemispheric dynamics and plasticity in clinical populations.

As a final note, it is important to consider the methodological limitations of the study. First, fNIRS has intrinsically lower spatial resolution than other neuroimaging techniques, such as fMRI, and the lack of individual anatomical images limits the precision in locating hemodynamic sources. Nevertheless, fNIRS offers several methodological advantages that are particularly relevant for the present study. Its fully non-invasive nature, tolerance to movement, and portability allow data collection in more ecological and flexible experimental settings,

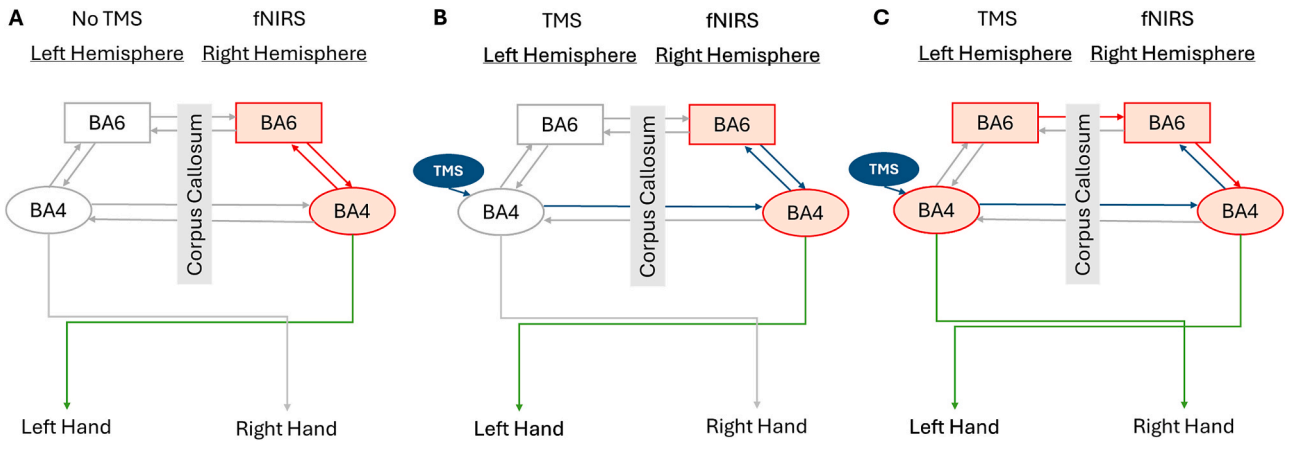

Fig. 9. A) No TMS condition: Right BA4 and BA6 are active during the isometric contraction of the left hand; BA4 and BA6 have reciprocal connections. B) TMS unimanual condition: Both right BA4 and BA6 are active during left hand isometric contraction; TMS on the left hemisphere induces inhibition via callosal pathways, leading to a reduction in the right BA4 activity; both right BA4 and BA6 activity is reduced, and the reduction in BA4 is correlated with the reduction in BA6. C) TMS bimanual condition: BA4 and BA6 of both hemispheres are active during isometric contraction of both hands; TMS on the left hemisphere induces inhibition via callosal pathways, leading to a reduction in right BA4. However, BA6 receives also a positive contribution from the left BA6 via callosal pathways. Red lines represent a positive influence from one area to another or an increase in activity, while blue lines indicate either an inhibitory effect from one area to another or a reduced contribution due to decreased activity in the connected area. Green and grey lines from BA4 to the hands indicate the presence or absence of motor activity, respectively. (For interpretation of the references to colour in this figure legend, the reader is referred to the web version of this article.)

including simultaneous use with TMS. Secondly, participants in the No TMS condition were not exposed to the auditory stimulus generated by the coil during the TMS conditions. This difference could be a confounding factor, as the presence of the sound associated with the TMS pulses could not be controlled in the comparison condition.

5. Conclusion

Our findings revealed a reduction in BA4 activity in the TMS unimanual and TMS bimanual conditions compared to the No TMS condition. Furthermore, we importantly observed that, besides primary motor cortex, a network of cortical regions is influenced by the transcallosal motor output. Notably, BA5 is highly correlated to iSP. All these findings expand the traditional models focused exclusively on BA4.

Data availability statement

The data that support the findings of this study are available from the corresponding author upon request.

Declaration of competing interest

The authors declare that they have no known competing financial interests or personal relationships that could have appeared to influence the work reported in this paper.

Acknowledgements

This research was supported by the Ministry of University and Research (MUR), National Recovery and Resilience Plan (NRRP), project MNESYS (PE0000006) A Multiscale integrated approach to the study of the nervous system in health and disease (D.D. n. 341 del 15/03/ 2022).

Appendix A. Supplementary data

Supplementary data to this article can be found online at https://doi.org/10.1016/j.clinph.2026.2111953.

References

Bajbouj, M., Gallinat, J., Niehaus, L., Lang, U.E., Roricht, S., Meyer, B.U., 2004. Abnormalities of inhibitory neuronal mechanisms in the motor cortex of patients with schizophrenia. Pharmacopsychiatry 37, 74–80.

Barker, J.W., Aarabi, A., Huppert, T.J., 2013. Autoregressive model based algorithm for correcting motion and serially correlated errors in fNIRS. Biomed. Opt. Express 4, 1366.

Bestmann, S., Baudewig, J., Siebner, H.R., Rothwell, J.C., Frahm, J., 2004. Functional MRI of the immediate impact of transcranial magnetic stimulation on cortical and subcortical motor circuits. Eur. J. Neurosci. 19, 1950–1962.

Bestmann, S., Swayne, O., Blankenburg, F., Ruff, C.C., Haggard, P., Weiskopf, N., Josephs, O., Driver, J., Rothwell, J.C., Ward, N.S., 2008. Dorsal premotor cortex exerts state-dependent causal influences on activity in contralateral primary motor and dorsal premotor cortex. Cereb. Cortex 18, 1281–1291.

Bonzano, L., Tacchino, A., Roccatagliata, L., Abbruzzese, G., Mancardi, G.L., Bove, M., 2008. Callosal contributions to simultaneous bimanual finger movements. J. Neurosci. Mar 19;28(12):3227-33.

Bonzano, L., Tacchino, A., Brichetto, G., Roccatagliata, L., Dessypris, A., Feraco, P., Lopes De Carvalho, M.L., Battaglia, M.A., Mancardi, G.L., Bove, M., 2014. Upper limb motor rehabilitation impacts white matter microstructure in multiple sclerosis. Neuroimage 90, 107–116.

Boroojerdi, B., Hungs, M., Mull, M., Töpper, R., Noth, J., 1998. Interhemispheric inhibition in patients with multiple sclerosis. Electroencephalogr. Clin. Neurophysiol. 109, 230–237.

Bortoletto, M., Bonzano, L., Zazio, A., Ferrari, C., Pedullà, L., Gasparotti, R., Miniussi, C., Bove, M., 2021. Asymmetric transcallosal conduction delay leads to finer bimanual coordination. Brain Stimul. 14, 379–388.

Curtin, A., Tong, S., Sun, J., Wang, J., Onaral, B., Ayaz, H., 2019. A systematic review of integrated functional near-infrared spectroscopy (fNIRS) and transcranial magnetic stimulation (TMS) studies. Front. Neurosci. 13.

Delpy, D.T., Cope, M., van der Zee, P., Arridge, S., Wray, S., Wyatt, J., 1988. Estimation of optical pathlength through tissue from direct time of flight measurement. Phys. Med. Biol. 33 (12), 1433–1442.

Di Lorenzo, R., Pirazzoli, L., Blasi, A., Bulgarelli, C., Hakuno, Y., Minagawa, Y., Brigadoi, S., 2019. Recommendations for motion correction of infant fNIRS data applicable to multiple data sets and acquisition systems. Neuroimage 200, 511–527.

Ehrsson, H.H., Fagergren, A., Jonsson, T., Westling, O., Johansson, R.S., Forssberg, H., Henrik, H., Westling, G., Forssberg Cortical, H., 2000. Cortical activity in precision- versus power-grip tasks: an fMRI study. J. Neurophysiol. 83 (1), 528–536.

Ferbert, A., Priori, A., Rothweel, J.C., Day, B.L., Colebatch, J.G., Marsden, C.D., 1992. Interhemispheric inhibition of the human motor cortex. J. Physiol. 453, 525–546.

Fox, P.T., Narayana, S., Tandon, N., Fox, S.P., Sandoval, H., Kochunov, P., Capaday, C., Lancaster, J.L., 2006. Intensity modulation of TMS-induced cortical excitation: primary motor cortex. Hum. Brain Mapp. 27, 478–487.

Giovannelli, F., Borgheresi, A., Balestrieri, F., Zaccara, G., Viggiano, M.P., Cincotta, M., Ziemann, U., 2009. Modulation of interhemispheric inhibition by volitional motor activity: an ipsilateral silent period study. J. Physiol. 587, 5393–5410.

Hupfeld, K.E., Swanson, C.W., Fling, B.W., Seidler, R.D., 2020. TMS-induced silent periods: a review of methods and call for consistency. J. Neurosci. Methods 346.

Huppert, T.J., Diamond, S.G., Franceschini, M.A., Boas, D.A., 2009. HomER: a review of time-series analysis methods for near-infrared spectroscopy of the brain. Appl. Opt. 48 (10), D280–D298.

Ilmoniemi, R., Virtanen, J., Ruohonen, J., Karhu, J., Aronen, H., Naatanen, R., Katila, T., 1997. Neuronal responses to magnetic stimulation reveal cortical reactivity and connectivity. Neuroreport 8 (16), 3537–3540.

Jung, P., Beyerle, A., Humpich, M., Neumann-Haefelin, T., Lanfermann, H., Ziemann, U., 2006. Ipsilateral silent period: a marker of callosal conduction abnormality in early relapsing-remitting multiple sclerosis? J. Neurol. Sci. 250, 133–139.

Kuhtz-Buschbeck, J.P., Gilster, R., Wolff, S., Ulmer, S., Siebner, H., Jansen, O., 2008. Brain activity is similar during precision and power gripping with light force: an fMRI study. Neuroimage 40, 1469–1481.

Laird, A.R., Robbins, J.M., Li, K., Price, L.R., Cykowski, M.D., Narayana, S., Laird, R.W., Franklin, C., Fox, P.T., 2008. Modeling motor connectivity using TMS/PET and structural equation modeling. Neuroimage 41, 424–436.

Lenzi, D., Conte, A., Mainero, C., Frasca, V., Fubelli, F., Totaro, P., Caramia, F., Inghilleri, M., Pozzilli, C., Pantano, P., 2007. Effect of corpus callosum damage on ipsilateral motor activation in patients with multiple sclerosis: a functional and anatomical study. Hum. Brain Mapp. 28, 636–644.

Manson, S.C., Palace, J., Frank, J.A., Matthews, P.M., 2006. Loss of interhemispheric inhibition in patients with multiple sclerosis is related to corpus callosum atrophy. Exp. Brain Res. 174, 728–733.

Makris, N., Kennedy, D.N., McInerney, S., Sorensen, A.G., Wang, R., Caviness, V.S., Pandya, D.N., 2005. Segmentation of subcomponents within the superior longitudinal fascicle in humans: a quantitative, in vivo, DT-MRI study. Cereb. Cortex 15, 854–869.

Meyer, B., Roricht, S., Woiciechowsky, C., 2004. Topography of fibers in the human corpus callosum mediating interhemispheric inhibition between the motor cortices. Ann. Neurol. 43, 360–369.

Meyer, B.-U., Roricht, S., Grafin von Einsiedel, H., Kruggel, F., Weindl, A., 1995. Inhibitory and excitatory interhemispheric transfers between motor cortical areas in normal humans and patients with abnormalities of the corpus callosum. Brain 118, 429–440.

Molavi, B., Dumont, G.A., 2012. Wavelet-based motion artifact removal for functional near-infrared spectroscopy. Physiol. Meas. 33, 259–270.

Momi, D., Wang, Z., Griffiths, J.D., 2023. TMS-evoked responses are driven by recurrent large-scale network dynamics. Elife 12.

Ortu, E., Deriu, F., Suppa, A., Tolu, E., Rothwell, J.C., 2008. Effects of volitional contraction on intracortical inhibition and facilitation in the human motor cortex. J. Physiol. 586, 5147–5159.

Padberg, J., Franca, J.G., Cooke, D.F., Soares, J.G.M., Rosa, M.G.P., Fiorani, M., Gattass, R., Krubitzer, L., 2007. Parallel evolution of cortical areas involved in skilled hand use. J. Neurosci. 27, 10106–10115.

Paus, T., Jech, R., Thompson, C.J., Comeau, R., Peters, T., Evans, A.C., 1997. Transcranial magnetic stimulation during positron emission tomography: a new method for studying connectivity of the human cerebral cortex. J. Neurosci. 17 (9), 3178–3184.

Perez, M.A., Butler, J.E., Taylor, J.L., 2014. Modulation of transcallosal inhibition by bilateral activation of agonist and antagonist proximal arm muscles. J. Neurophysiol. 111, 405–414.

Perez, M.A., Cohen, L.G., 2008. Mechanisms underlying functional changes in the primary motor cortex ipsilateral to an active hand. J. Neurosci. 28, 5631–5640.

Premji, A., Rai, N., Nelson, A., 2011. Area 5 influences excitability within the primary motor cortex in humans. PLoS One 6.

Rocca, M.A., Valsasina, P., Martinelli, V., Misci, P., Falini, A., Comi, G., Filippi, M., 2012. Large-scale neuronal network dysfunction in relapsing-remitting multiple sclerosis.

Sarfeld, A.S., Diekhoff, S., Wang, L.E., Liuzzi, G., Uludağ, K., Eickhoff, S.B., Fink, G.R., Grefkes, C., 2012. Convergence of human brain mapping tools: neuronavigated TMS parameters and fMRI activity in the hand motor area. Hum. Brain Mapp. 33, 1107–1123.

Schmierer, K., Niehaus, L., Röricht, S., Meyer, B.-U., 2000. Conduction deficits of callosal fibres in early multiple sclerosis. J. Neurol. Neurosurg. Psychiatry 68 (5), 633–638.

Scholkmann, F., Spichtig, S., Muehlemann, T., Wolf, M., 2010. How to detect and reduce movement artifacts in near-infrared imaging using moving standard deviation and spline interpolation. Physiol. Meas. 31, 649–662.

Scholkmann, F., Wolf, M., 2013. General equation for the differential pathlength factor of the frontal human head depending on wavelength and age. J. Biomed. Opt. 18, 105004.

Siebner, H.R., Funke, K., Aberra, A.S., Antal, A., Bestmann, S., Chen, R., et al., 2022. Transcranial magnetic stimulation of the brain: what is stimulated? – a consensus and critical position paper. Clin. Neurophysiol. 140, 59–97.

Siebner, H.R., Peller, M., Willoch, F., Auer, C., Bartenstein, P., Drzezga, A., Schwaiger, M., Conrad, B., 1999. (1999) Imaging functional activation of the

auditory cortex during focal repetitive transcranial magnetic stimulation of the primary motor cortex in normal subjects. Neurosci. Lett. 270 (1), 37–40.
Siebner, H.R., Willoch, F., Peller, M., Auer, C., Boecker, H., Conrad, B., Bartenstein, P., 1998. Imaging brain activation induced by long trains of repetitive transcranial magnetic stimulation. Neuroreport 1998; 9(5), 943-948.
Sohn, Y.H., Jung, H.Y., Kaelin-Lang, A., Hallett, M., 2003. Excitability of the ipsilateral motor cortex during phasic voluntary hand movement. Exp. Brain Res. 148, 176–185.
Soteropoulos, D.S., Perez, M.A., 2011. Physiological changes underlying bilateral isometric arm voluntary contractions in healthy humans. J. Neurophysiol. 105, 1594–1602.
Stinear, J.W., Byblow, W.D., 2004. Modulation of human cervical premotoneurons during bilateral voluntary contraction of upper-limb muscles. Muscle Nerve 29, 506–514.
Trompetto, C., Bove, M., Marinelli, L., Avanzino, L., Buccolieri, A., Abbruzzese, G., 2004. Suppression of the transcallosal motor output: a transcranial magnetic stimulation study in healthy subjects. Exp. Brain Res. 158, 133–140.
Van Duinen, H., Renken, R., Maurits, N.M., Zijdewind, I., 2008. Relation between muscle and brain activity during isometric contractions of the first dorsal interosseus muscle. Hum. Brain Mapp. 29 (3), 281–299.
Wassermann, E.M., Fuhr, P., Cohen, G., Hallett, M., 1991. (1991) Effects of transcranial magnetic stimulation on ipsilateral muscles. Neurology 41 (11), 1795.
Yücel, M.A., Selb, J., Cooper, R.J., Boas, D.A., 2014. Targeted principle component analysis: a new motion artifact correction approach for near-infrared spectroscopy. J. Innov. Opt. Health Sci. 7.
Zimeo Morais, G.A., Balardin, J.B., Sato, J.R., 2018. FNIRS Optodes' Location Decider (fOLD): a toolbox for probe arrangement guided by brain regions-of-interest. Sci. Rep. 8.